J. Opt. A: Pure Appl. Opt. **11** (2009) 114007 (8pp) doi:10.1088/1464-4258/11/11/114007

Fluorescence signal of a single emitter coupled to a nanoparticle through a plasmonic film

C Vandenbem[1,2], L S Froufe-Pérez[3] and R Carminati[1]

[1] Institut Langevin, ESPCI, CNRS UMR 7587, Laboratoire d'Optique Physique, 10 rue Vauquelin, F-75231 Paris Cedex 05, France
[2] Research Center in Physics of Matter and Radiation (PMR), University of Namur (FUNDP), 61 rue de Bruxelles, B-5000 Namur, Belgium
[3] Instituto de Ciencia de Materiales de Madrid, CSIC, Cantoblanco, E-28049 Madrid, Spain

E-mail: remi.carminati@espci.fr

Received 30 January 2009, accepted for publication 23 April 2009
Published 16 September 2009
Online at stacks.iop.org/JOptA/11/114007

Abstract
We study theoretically the detection of the fluorescence intensity emitted by a single emitter coupled to a nanoparticle through a metallic thin film. The coupling results from the overlap of the surface plasmon modes propagating on each interface of the film. We show that the distance between the nanoparticle and the film can be used to tune the apparent quantum yield and the radiation pattern with nanometer-scale sensitivity. Such a system is appealing from the experimental point of view since it involves simple structures that can be controlled using current scanning near-field optical techniques. It could be used to improve the detection sensitivity of molecules embedded in substrates, or to design sensitive biological or chemical plasmonic sensors.

Keywords: fluorescence, single molecule, plasmons, quenching, molecular imaging

(Some figures in this article are in colour only in the electronic version)

1. Introduction

Bringing sharp metallic tips or nanoparticles, commonly denoted as nanoantennas, in the near-field of single emitters (e.g. molecules, quantum dots) can substantially modify the lifetime and the fluorescence signal of these emitters, leading to fluorescence enhancement or quenching. Several effects of the nanoantennas can be identified: an enhancement of the local field [1, 2], a modification of the spontaneous emission rate (Purcell effect [3, 4]) and an angular redistribution of the radiation emission [5–7]. When using metallic objects, the fluorescence signal is affected by the coupling with radiative and non-radiative decay channels [8], and the competition between them reduces the fluorescence enhancement capability [7, 9, 10]. Usually, metallic nanostructures are considered as good candidates to control the dynamics of single emitters on the nanometer scale. Nevertheless, the interaction between electromagnetic modes and molecules can also be used to influence polariton transfer along devices, for example, for signal multiplexing applications [11].

Recently, a scheme has been proposed in order to act on a single molecule at distances >100 nm with high spatial sensitivity [12]. The scheme involves a metallic nanoparticle coupled to the emitter through a plasmonic film, made of a metallic or a negative-index material, working in the so-called 'superlens' regime [13, 14]. In this scheme, the emitter couples efficiently to surface plasmon polaritons that propagate on both sides of the film. In the case of a single film, this coupling has been observed experimentally and is responsible for the enhanced transmission of the fluorescence signal through a corrugated thin metal film [15] or continuous gold film [16]. By bringing a metallic nanoparticle on the other side of the film, the fluorescence lifetime of the emitter can be substantially modified [12]. The mechanism relies chiefly on the non-radiative coupling between the emitter and

the nanoparticle that is induced by surface plasmons. In that sense, the situation is similar to that described in [17], in which plasmon modes of silver films were used to increase the interaction between donors and acceptors placed on opposite sides of the film. Fluorescence resonance energy transfer (FRET) was observed far beyond the usual Förster radius [18], up to distances of 120 nm. Finally, we note that the mechanism should occur at any frequency for which surface plasmons are excited, and not only at the frequency that induces the superlens behavior of the film.

In view of a practical implementation of the film–nanoparticle scheme, one should study the fluorescence intensity (and not only the lifetime), which depends on the illumination conditions and on the apparent quantum yield of the coupled system. A key point is to discern under which conditions the fluorescence signal can be optimized, in terms of intensity and/or angular distribution. It is the purpose of this work to address this issue. We present a theoretical study of the fluorescence signal emitted by a single fluorophore coupled to a single nanoparticle through a metallic thin film, based on rigorous three-dimensional numerical simulations. In order to focus on a specific example, we have considered that the nanoparticle and the film are both made of silver. The nanoparticle is assumed to be attached, for example, at the end of a near-field probe, so that it can be scanned at nanometer distance from the film surface. The results are that the apparent quantum yield and the radiation pattern can be tuned by changing the distance between the nanoparticle and the film, with nanometer-scale sensitivity. In particular, in the presence of the nanoparticle, the signal can be either enhanced or reduced with respect to the signal in the presence of the film alone. From the experimental point of view, the system is appealing since it involves simple structures which can be controlled using current scanning near-field optical techniques.

2. Fluorescence signal

We consider a single dipole emitter, with emission frequency ω, located at a position $\mathbf{r}_s$ in the vicinity of a metallic object. The normalized spontaneous decay rate Γ/Γ_0, where Γ_0 is the decay rate in vacuum, is proportional to the imaginary part of the electric-field susceptibility (the Green function) which describes the electromagnetic response of the environment [19, 20]:

$$\frac{\Gamma}{\Gamma_0} = 1 + \frac{6\pi\epsilon_0}{k^3}\mathrm{Im}\,[\mathbf{u}\cdot\mathbf{G}_s(\mathbf{r}_s,\mathbf{r}_s,\omega)\cdot\mathbf{u}] \tag{1}$$

where $k = \omega/c$, with c the speed of light in vacuum and $\mathbf{u}$ is a unit vector in the direction of the transition dipole. The dyadic $\mathbf{G}_s$ describes the modification of the free-space dyadic Green function $\mathbf{G}_0$ due to the presence of the object (in our case the slab–nanoparticle system). Note that $\tau = 1/\Gamma$ is the fluorescence lifetime.

The spontaneous decay can occur though radiative channels (emission of a photon) or non-radiative channels (absorption). In the classical picture, in which the transition dipole $\mathbf{p}$ of the fluorescent emitter is treated as a classical harmonic damped electric dipole, the radiative decay rate Γ^R is proportional to the far-field radiated power and the non-radiative decay rate Γ^{NR} is proportional to the power absorbed by the environment. Energy conservation requires that $\Gamma = \Gamma^R + \Gamma^{NR}$, so that only two quantities need to be calculated. The apparent quantum yield of the emitter, in the presence of the object, is defined by

$$\eta = \frac{\Gamma^R}{\Gamma^R + \Gamma^{NR}}. \tag{2}$$

We have assumed for simplicity that the intrinsic quantum yield of the free emitter is unity (which means that Γ^{NR} results from additional non-radiative decay channels induced by the environment). The apparent quantum yield η is an important quantity that drives the fluorescence signal. Small values of η, due to substantial non-radiative coupling, can lead to fluorescence quenching. Indeed, in the non-saturated regime, the fluorescence signal can be written [21]

$$S = C\,\eta(\omega)\,\sigma_{abs}(\omega_{abs})|K(\omega_{abs})|^2 I_{exc}(\omega_{abs})\,T \tag{3}$$

where ω_{abs} and ω are the absorption and emission frequencies of the molecule, respectively, $\sigma_{abs}(\omega_{abs})$ is the absorption cross section of the free molecule in vacuum, $I_{exc}(\omega_{abs})$ is the intensity of the exciting beam in the absence of the object and T is the integration time of the detector. The local-field factor $K(\omega_{abs})$ is defined by $|\mathbf{E}_{loc}(\omega_{abs})| = K(\omega_{abs})|\mathbf{E}_{exc}(\omega_{abs})|$ with $\mathbf{E}_{loc}$ the local field at the molecule's location in the presence of the object and $\mathbf{E}_{exc}$ the exciting field in vacuum [$I_{exc}(\omega_{abs}) = |\mathbf{E}_{exc}(\omega_{abs})|^2$]. The constant C is a factor that depends on the detection geometry and the efficiency of the detector. For simplicity, we shall assume a two-level emitter for which $\omega_{abs} = \omega$ (in practice, this approximation is valid as long as the Stokes shift $\omega_{abs} - \omega$ remains smaller than the spectral width of the resonances of the object). In order to characterize the regimes of fluorescence enhancement or quenching, it is convenient to cast the fluorescence signal in the form

$$S = \eta(\omega)|K(\omega_{abs})|^2 S_{vac} \tag{4}$$

where $S_{vac} = C\,\sigma_{abs}(\omega_{abs})I_{exc}(\omega_{abs})\,T$ is the fluorescence signal of the free emitter in vacuum. This expression shows that the product $\eta(\omega)|K(\omega)|^2$ is the key quantity: $\eta(\omega)|K(\omega)|^2 > 1$ corresponds to fluorescence enhancement and $\eta(\omega)|K(\omega)|^2 \ll 1$ to fluorescence quenching.

A few remarks must be made at this point. Equation (4) has been obtained in the weak coupling regime, in which local fields are proportional to the exciting field and the effects of field gradients are neglected. The latter are relevant if the local field varies considerably on length scales of the order of the emitter dimensions (typically a few ångströms) [22]. In the situations considered in this work, field gradients are, as such, an order of magnitude smaller. Moreover, when the distance between metallic objects and the emitter reaches a few nanometers, non-local effects may play an important role [23, 24]. With silver surfaces, we have shown [25] that the influence of non-local effects on the fluorescence decay rate can be neglected for distances between the emitter and the metal surface $z_s \gtrsim 3$ nm. We will therefore neglect field-gradient and non-local effects throughout this work.

3. Computation of Green functions

The calculation of the fluorescence signal relies on the numerical evaluation of the Green function of the full nanoparticle–slab system. Indeed, the spontaneous decay rate can be computed from (1), the apparent quantum yield can be deduced from a calculation of the far-field radiated power (which is known once the total radiated field is calculated) and the local-field factor can be obtained by computing the field scattered by the nanoparticle–slab system illuminated by a plane wave. The Green function $\mathbf{G}$ of the nanoparticle–slab system connects a classical electric dipole $\mathbf{p}$ at position $\mathbf{r}_s$ to the radiated electric field at position $\mathbf{r}$ through the relation $\mathbf{E}(\mathbf{r}, \omega) = \mathbf{G}(\mathbf{r}, \mathbf{r}_s, \omega) \cdot \mathbf{p}$. It takes the form

$$\mathbf{G}(\mathbf{r}, \mathbf{r}_s, \omega) = \mathbf{G}_0(\mathbf{r}, \mathbf{r}_s, \omega) + \mathbf{G}_s(\mathbf{r}, \mathbf{r}_s, \omega). \quad (5)$$

Since the free-space Green function $\mathbf{G}_0$ is known analytically, we only need to compute numerically $\mathbf{G}_s(\mathbf{r}, \mathbf{r}_s, \omega)$, i.e. the modification of the Green function induced by the slab–nanoparticle system [12]. The Green function of an isolated slab has an analytical expression in Fourier space (angular spectral decomposition) [26]. Infinite interfaces are described exactly in this formalism through Fresnel reflection and transmission coefficients. In particular, surface electromagnetic modes are accounted for without any approximation. In order to include the additional scattering induced by the nanoparticle, we use the discrete dipole approximation (DDA) [27, 28]. The spherical nanoparticle is discretized in a set of N small spheres (unit cells) that are treated in the electric dipole approximation. The field scattered by each unit cell is calculated using the Green tensor of the slab. The approach is similar to that used in [29]. Note that the polarizability $\alpha(\omega)$ of each cell is obtained by taking into account the effect of the slab, and fully includes the radiation reaction. Hence, the optical theorem is exactly verified. Coupling between induced dipoles in all unit cells leads to a linear system of coupled equations, involving the polarizabilities, the free-space Green function and the Green function of the slab [12]. The linear system is solved numerically and provides the self-consistent induced dipole moments in each unit cell. The scattered field can be readily calculated at any position in space, as the field radiated by each induced dipole in the presence of the slab. Let us mention that the method is developed for three-dimensional geometries and that it includes far-field and near-field multiple scattering between the slab interfaces and the nanoparticle. We also stress that, although the influence of the slab is taken into account analytically through the Green function, additional scattering from surface roughness and grain boundaries in the slab is not included in the present work. Its influence is expected to be a lowering in the field enhancement and a reduction of the lateral resolution of any potential local probe application.

4. Results

The geometry is schematically represented in figure 1. The dipole emitter (fluorescent molecule) lies below a silver film of width L. The z axis is perpendicular to the slab interface.

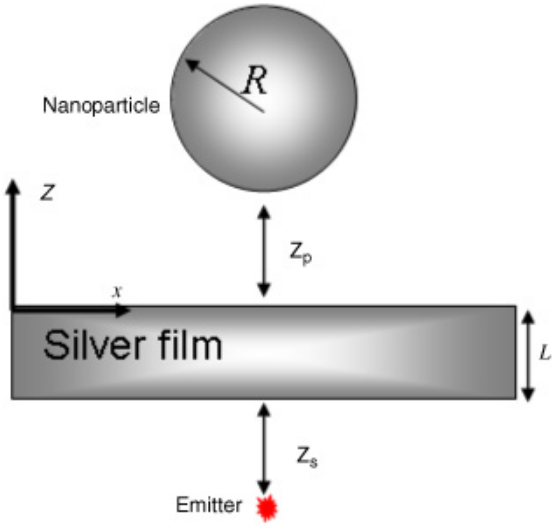

Figure 1. Geometry of the system. A silver nanoparticle couples to a single emitter through a silver film.

The emitter is placed at a distance z_s from the lower interface of the slab. A silver nanoparticle with radius R is placed on the other side of the slab. The surface-to-surface distance between the nanoparticle and the slab is denoted by z_p. The lateral extension of the film along the x and y directions is infinite. We have chosen to compute the fluorescence signal for two different excitation–emission wavelengths: $\lambda = 354$ nm (corresponding to the localized plasmon resonance of the nanoparticle) and $\lambda = 337$ nm (corresponding to the surface plasmon resonance of the film).

4.1. Sphere on-resonance

We consider a nanoparticle with radius $R = 10$ nm (discretized with $N = 43$ dipoles in the DDA calculation). At the wavelength $\lambda = 354$ nm, the bulk value of the permittivity of silver is $\epsilon = -2.03+0.6\mathrm{i}$ [30], so that the nanoparticle is excited at resonance (with $R \ll \lambda$, the nanoparticle behaves as an electric dipole and the plasmon resonance corresponds to $\mathrm{Re}(\epsilon) \simeq -2$). The emitter is located at $z_s = 10$ nm below the slab and its transition dipole is oriented along the z direction. The film thickness is $L = 10$ nm. We show in figure 2 the dependence of the radiative and the non-radiative decay rates on the nanoparticle–slab distance z_p. For the sake of comparison, we represent the decay rates of the full nanoparticle–film system normalized by the decay rates in the presence of the film alone.

The normalized non-radiative decay rate Γ^{NR} decreases at short distance. As we have mentioned before, the non-radiative contribution results from absorption in metals. For small z_p, the nanoparticle and the slab are coupled. This coupling yields a new spatial distribution of the field. Instead of being localized inside metals, the electric field tends to concentrate in the vacuum gap between the nanoparticle and the slab surface, so that absorption is reduced. Interestingly, the increase in the coupling strength between the emitter and the nanoparticle gives rise to an enhancement of the radiative decay rate Γ^{R}. The radiated power increases by a factor of 2 for $z_p = 5$ nm. For z_p larger than 50 nm, the interaction between the sphere

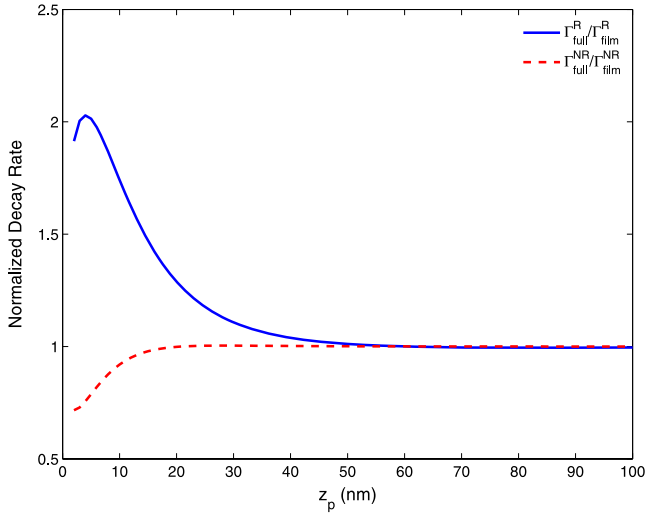

Figure 2. Influence of the sphere location z_p on the normalized radiative decay rate (——) and non-radiative decay rate (- - - -). The emitter is placed near the silver film, with a silver sphere of radius $R = 10$ nm on the other side. The dipole emits at a wavelength $\lambda = 354$ nm, is located at $z_s = 10$ nm and is oriented along the z axis.

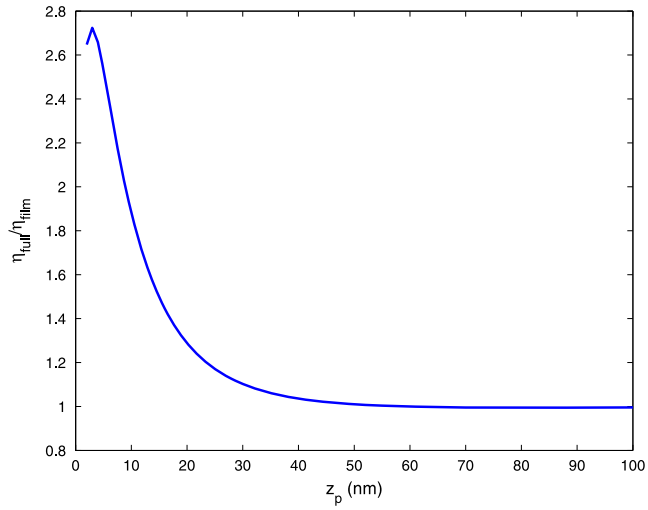

Figure 3. Influence of the sphere location z_p on the normalized apparent quantum yield. The emitter is placed near the silver film, with a silver sphere of radius $R = 10$ nm on the other side. The dipole emits at a wavelength $\lambda = 354$ nm, is located at $z_s = 10$ nm and is oriented along the z axis.

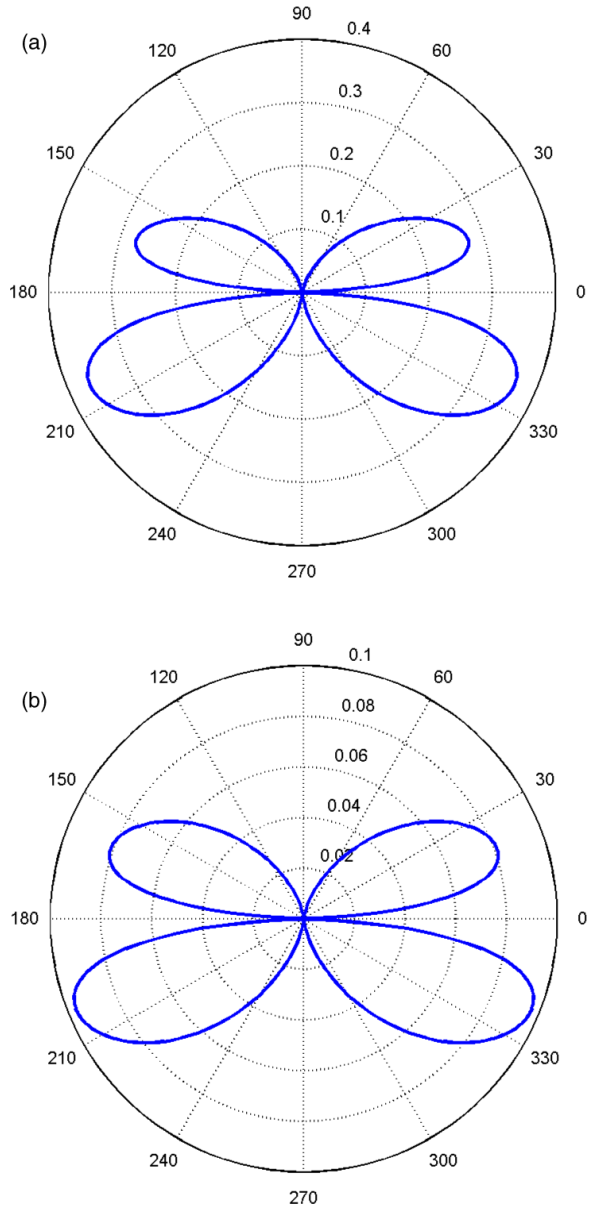

Figure 4. Radiation pattern versus the observation angle for an emitter close to a silver film with thickness $L = 10$ nm. The dipole emits at a wavelength $\lambda = 354$ nm, is located at $z_s = 10$ nm and is oriented along the z axis. (a) Full nanoparticle–film system with $z_p = 10$ nm. (b) Film alone.

and the thin film vanishes. The decay rates of the full system and the decay rates of the isolated film coincide.

The opposite variations of the radiative and the non-radiative decay rates induce a peculiar behavior of the apparent quantum yield. As seen in figure 3, for $z_p = 3$ nm, the quantum yield of the full nanoparticle–film system is 2.7 times larger than the quantum yield of the isolated film. This means that, by bringing the metallic nanoparticle close to the film surface, one increases the apparent quantum yield, which is not an intuitive behavior.

For the characterization of the fluorescence signal, the apparent quantum yield is not the only relevant quantity. The other key factor is the local-field factor, which describes the enhancement of the local exciting intensity through the factor $|K|^2$. The amplitude of the local-field factor is expected to depend strongly on the illumination direction. Indeed, it is known that the emission pattern of a single emitter can be modified by the environment, e.g. by a near-field probe [6]. According to the reciprocity theorem [31], a preferential direction of emission (given by a lobe of emission) also corresponds to an illumination direction leading to an enhanced local-field factor. For that purpose, we have computed the emission diagram of the emitter in the presence of the system. The emission diagram is defined as the angular distribution of the intensity radiated into the far-field by a classical point dipole placed at the location of the emitter. The result is shown in figure 4. The emission diagram of the full system

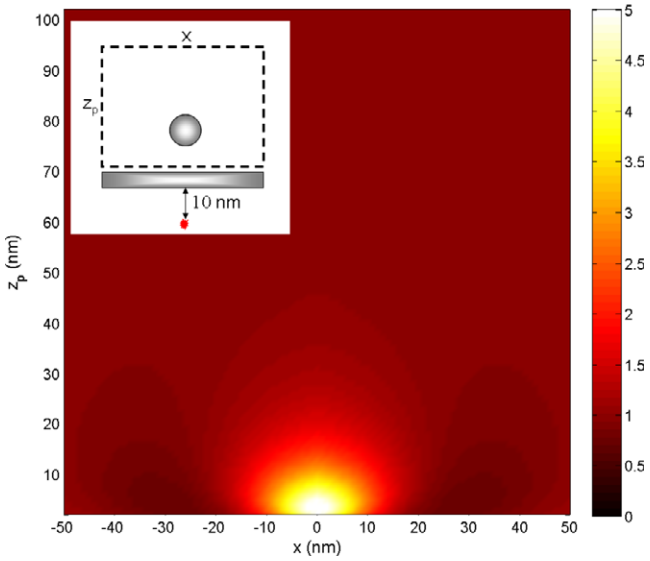

Figure 5. Fluorescence signal $S_{\text{full}}/S_{\text{film}}$ for an emitter near a silver film with thickness $L = 10$ nm versus the position of a nanoparticle scanning a rectangular region on the other side of the film. The scanning region is represented in the inset. The dipole emits at a wavelength $\lambda = 354$ nm, is located at $z_s = 10$ nm and is oriented along the z axis.

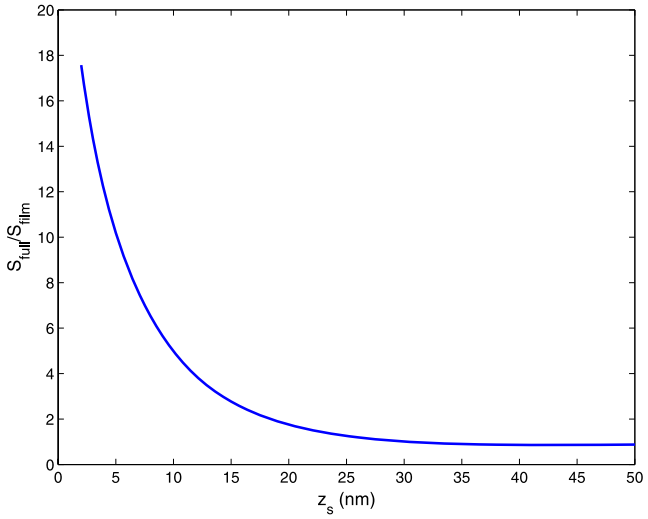

Figure 6. Influence of source location z_s on the fluorescence signal $S_{\text{full}}/S_{\text{film}}$ of an emitter near a silver film with thickness $L = 10$ nm, in the presence of a silver nanosphere of radius $R = 10$ nm, placed on the other side of the film at a distance $z_p = 5$ nm. The dipole emits at a wavelength $\lambda = 354$ nm and is oriented along the z axis.

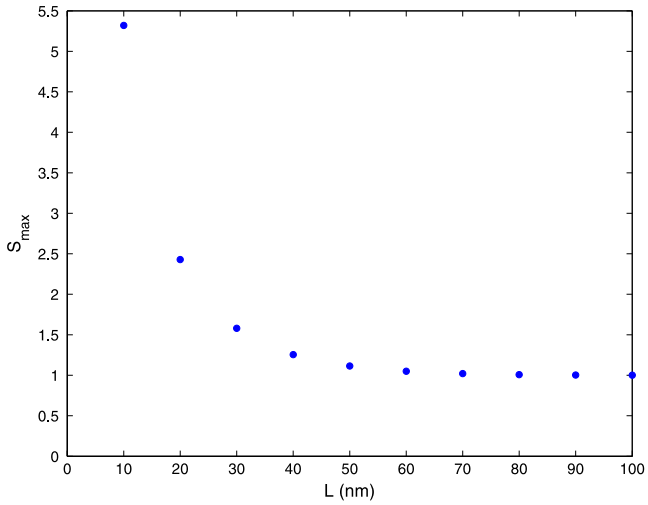

Figure 7. Influence of film thickness L on the maximum S_{max} of the normalized fluorescence signal. The emitter is placed near the silver film, with a silver sphere of radius $R = 10$ nm on the other side. The dipole emits at a wavelength $\lambda = 354$ nm, is located at $z_s = 10$ nm and is oriented along the z axis.

(figure 4(a)) gives us two pieces of information. First, part of the energy emitted by the dipole is transferred to the opposite side of the slab, where the nanoparticle stands (0°–180°). Second, there are two preferential directions for the exciting beam (assumed here to be a plane wave): one above the slab (corresponding to an incidence angle of 20°), and one below the slab (corresponding to an angle of −25°).

We now turn to the study of the fluorescence signal. We assume a configuration with a directional (plane wave) excitation and a detection of all emitted photons (the signal is integrated over the detection directions). We choose a specific illumination direction (20°), which determines the local-field factor K, and compute the fluorescence signal versus the position z_p of the nanoparticle. The distance between the emitter and the lower surface of the slab is kept constant at the value $z_s = 10$ nm. While the nanoparticle scans a square region above the metallic film, we compute the normalized fluorescence signal $S_{\text{full}}/S_{\text{film}}$, i.e. the ratio between the signal in the presence of the full nanoparticle–film system and the signal in the presence of the film alone. The result is displayed in figure 5. Note that taking the fluorescence intensity in the presence of the film alone as a reference allows us to visualize directly the influence of the nanoparticle and to compare with previous experimental studies of fluorescence emission close to isolated slabs [16, 17]. In the present situation, the interaction between the plasmonic resonance of the nanosphere and the surface mode of the thin film increases the fluorescence intensity, compared to the situation of the film alone. For very small distances ($z_p < 10$ nm), the enhancement is of the order of 4.

We show in figure 6 the normalized fluorescence signal $S_{\text{full}}/S_{\text{film}}$ versus the distance z_s between the molecule and the surface of the slab, for a fixed position $z_p = 5$ nm of the nanoparticle. We observe that the signal increases at short distance, to reach a value of 17 for $z_s = 3$ nm (below this distance, we assume that our model is no longer valid). For $z_s > 30$ nm, no enhancement is observed, so that the presence of the nanoparticle does not influence the emitter–film system.

In order to determine the influence of the film thickness, we define S_{max} as the maximum value of the normalized fluorescence signal $S_{\text{full}}/S_{\text{film}}$ in a map such as that shown in figure 5. By changing the film thickness, and computing maps with all other parameters unchanged, one can follow the evolution of S_{max}. The result is shown in figure 7. The maximum of the fluorescence signal decreases rapidly with the

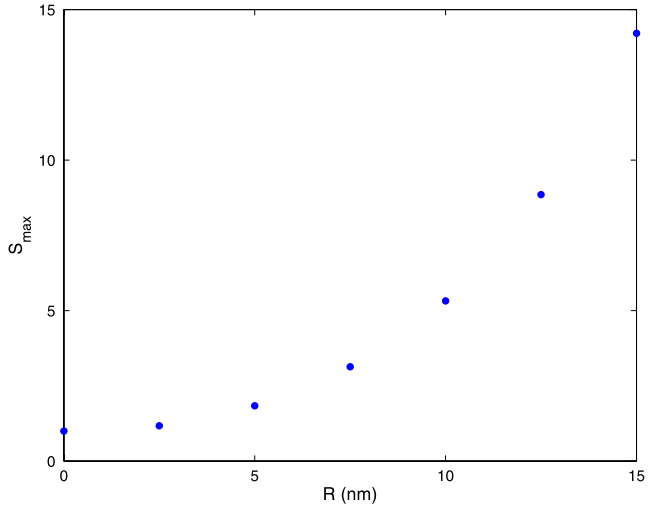

Figure 8. Influence of the size of the nanoparticle on the fluorescence signal of an emitter near a silver sphere of radius R and a silver film with thickness $L = 10$ nm. The dipole emits at a wavelength $\lambda = 354$ nm, is located at $z_s = 10$ nm and is oriented along the z axis.

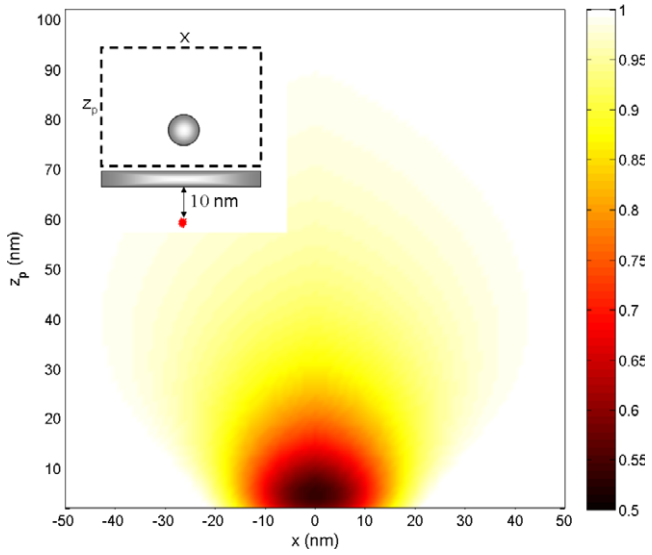

Figure 9. Fluorescence signal S_{full}/S_{film} for an emitter near a silver film with thickness $L = 10$ nm versus the position of a nanoparticle scanning a rectangular region on the other side of the film. The scanning region is represented in the inset. The dipole emits at a wavelength $\lambda = 337$ nm, is located at $z_s = 10$ nm and is oriented along the z axis.

film thickness, due to the reduction of the coupling strength of the plasmon modes on both sides of the film.

Finally, we calculate the maximum of the normalized signal S_{max} versus the radius of the nanoparticle (in the range 0–15 nm). The result, shown in figure 8, reveals that the larger the particle, the higher the enhancement of the fluorescence signal. The variation follows a kind of exponential law.

4.2. Film on-resonance

In this section, we choose a wavelength corresponding to the resonant excitation of surface modes on the film interfaces. This wavelength corresponds to $\mathrm{Re}(\epsilon) \approx -1$. At the wavelength $\lambda = 337$ nm, the permittivity of silver is equal to $\epsilon = -1.005+0.583\mathrm{i}$ [30], so that one is very close to the resonance condition. In the following calculations, the emitter is placed at a distance $z_s = 10$ nm from the lower film surface and the transition dipole is oriented along the z direction. We consider a nanoparticle with radius $R = 10$ nm and a film with thickness $L = 10$ nm.

The normalized fluorescence signal S_{full}/S_{film} is presented in figure 9. As in figure 5, the nanoparticle scans a square region above the film (see the inset for a schematic view). We choose an angle of illumination of 40° that was deduced from the radiation pattern of the emitter (not shown for brevity). We see that the fluorescence signal is quenched for this wavelength of excitation when we approach the sphere close to the film. The sphere does not improve the fluorescence signal in comparison with the film alone because there is no delocalization of the field in the vacuum gap between the nanosphere and the slab surface. The coupling between the emitter and the sphere is, in consequence, relatively weak. In addition, we have computed the normalized radiative and non-radiative decay rates (figure 10). The radiative decay rate presents a minimum for $z_p = 7$ nm. For the same distances,

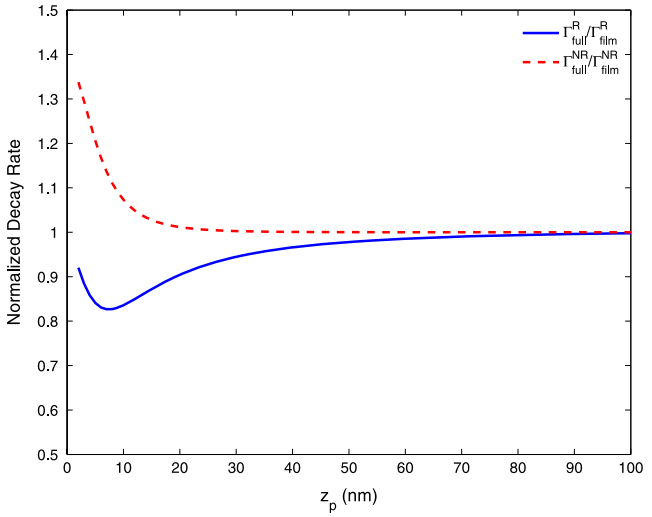

Figure 10. Influence of the sphere location z_p on the normalized radiative decay rate (——) and non-radiative decay rate (- - - -). The emitter is placed near the silver film, with a silver sphere of radius $R = 10$ nm on the other side. The dipole emits at a wavelength $\lambda = 337$ nm, is located at $z_s = 10$ nm and is oriented along the z axis.

the absorption in the system increases. Thus, the apparent quantum yield of the emitter decreases drastically (not shown for brevity). For these specific parameters, the spontaneous decay rate is mainly driven by the non-radiative decay rate.

4.3. Remarks

Before drawing some conclusions, we want to add two comments. Although not shown for the sake of brevity, we have verified that a silver system excited off-resonance

($\lambda = 612$ nm, $\epsilon = -15.4+1.02$i [30]) does not lead to any significant fluorescence enhancement. The radiation pattern is slightly modified. The best angles of illumination are 10° and −22°.

A remaining question is the influence of the bulk material. From the experimental point of view, gold is usually more suitable. However, gold is a more absorbing metal in comparison with silver in the visible. At the localized plasmon resonance wavelength ($\lambda = 498$ nm), the bulk permittivity of gold is $\epsilon = -2.335+3.61$i [30]. We still observe an enhancement of the fluorescence signal with the nanoparticle (not shown for brevity). For instance, with a sphere of $R = 10$ nm, a film of $L = 10$ nm and a source located at $z_s = 10$ nm, the gain reaches a maximal value of 1.6.

5. Conclusion

We have investigated theoretically the coupling of a single fluorescent emitter to a nanoparticle through a metallic film. The coupling mechanism underneath is due to the overlap between the two surface plasmon modes that propagate at each interface of the film as shown in detail in [12]. In the present study, we have focused on the characterization of the fluorescence signal. We have shown that the apparent quantum yield and the radiation pattern of a single emitter can be tuned with nanometer-scale sensitivity, by changing the nanoparticle–film distance. In particular, in the presence of the nanoparticle, the signal can be either enhanced or reduced with respect to the signal in the presence of the film alone.

In view of designing an experimental set-up, both the sphere and the thin film were assumed to be made of silver. The radius of the nanoparticle was fixed to 10 nm. Exciting the localized plasmon of the sphere ($\lambda = 354$ nm) is the most attractive case for the enhancement of the fluorescence intensity. A strong coupling between the emitter and the nanoparticle occurs through the film. The thickness of the silver thin film influences the radiative output of the single emitter. With a film of a thickness of 10 nm, we gain a factor of 5 in the fluorescence intensity when approaching the sphere in the vicinity of the slab. For thicknesses up to 80 nm, the nanoparticle still improves the fluorescence intensity (10%). In addition to a substantial enhancement of the fluorescence signal, we have noticed that the sphere/film system influences the emitter radiation pattern more in amplitude than in direction. From the experimental point of view, the configuration is appealing since it involves simple structures which can be controlled using current scanning near-field optical techniques. It could be used to improve the detection sensitivity of molecules embedded in substrates or to design sensitive biological or chemical plasmonic sensors.

Acknowledgments

This work was supported by the EU Projects ‘Molecular Imaging’ under contract no. LSHG-CT-2003-503259 and ‘Nanomagma’ under contract FP7-NMP-2007-SMALL-1. CV is a postdoctoral researcher of the Belgian National Fund for Scientific Research (FRS-FNRS) and acknowledges a grant from the City of Paris that made possible a stay at ESPCI where this work was done. LSFP acknowledges the financial support of the Spanish Ministry of Science and Innovation through its Juan de la Cierva program.

References

[1] Hecht B, Bielefeldt H, Novotny L, Inouye Y and Pohl D W 1996 Local excitation, scattering, and interference of surface plasmons *Phys. Rev. Lett.* **77** 1889
[2] Foteinopoulou S, Vigneron J P and Vandenbem C 2007 Optical near-field excitations on plasmonic nanoparticle-based structures *Opt. Express* **15** 4253
[3] Purcell E M 1946 Spontaneous emission probabilities at radio frequencies *Phys. Rev.* **69** 681
[4] Barnes W L 1998 Fluorescence near interfaces: the role of photonic mode density *J. Mod. Opt.* **45** 661
[5] Betzig E and Chichester R J 1993 Single molecules observed by near-field scanning optical microscopy *Science* **262** 1422
[6] Gersen H, Garcia-Parajo M F, Novotny L, Veerman J A, Kuipers L and van Hulst N F 2000 Influencing the angular emission of a single molecule *Phys. Rev. Lett.* **85** 5312
[7] Thomas M, Greffet J-J, Carminati R and Arias-Gonzales J R 2004 Single molecule spontaneous emission close to absorbing structures *Appl. Phys. Lett.* **85** 3863
[8] Carminati R, Greffet J J, Henkel C and Vigoureux J M 2006 Radiative and non-radiative decay rate of a single molecule close to a metallic nanoparticle *Opt. Commun.* **261** 368
[9] Anger P, Bharadwaj P and Novotny L 2006 Enhancement and quenching of single-molecule fluorescence *Phys. Rev. Lett.* **96** 113002
[10] Kühn S, Håkanson U, Rogobete L and Sandoghdar V 2006 Enhancement of single-molecule fluorescence using a gold nanoparticle as an optical nanoantenna *Phys. Rev. Lett.* **97** 017402
[11] Neuhauser D and Lopata K 2007 Molecular nanopolaritonics: cross manipulation of near-field plasmons and molecules. I. Theory and application to junction control *J. Chem. Phys.* **127** 154715
[12] Froufe-Pérez L S and Carminati R 2008 Controlling the fluorescence lifetime of a single emitter on the nanoscale using a plasmonic superlens *Phys. Rev.* B **78** 125403
[13] Fang N, Lee H, Sun C and Zhang X 2005 Subdiffraction-limited optical imaging with a silver superlens *Science* **308** 354
[14] Taubner T, Korobkin D, Urzhumov Y, Schvets G and Hillenbrand R 2006 Near-field microscopy through a SiC superlens *Science* **313** 1565
[15] Gruhlke R W, Holland W R and Hall D G 1986 Surface plasmon cross coupling in molecular fluorescence near a corrugated thin metal film *Phys. Rev. Lett.* **56** 2838
[16] Stefani F D, Vasilev K, Bocchio N, Stoyanova N and Kreiter M 2005 Surface-plasmon-mediated single-molecule fluorescence through a thin metallic film *Phys. Rev. Lett.* **94** 023005
[17] Andrew P and Barnes W L 2004 Energy transfer across a metal film mediated by surface plasmon polaritons *Science* **306** 1002
[18] Förster T 1948 Zwischenmolekulare energiewanderung und fluoreszenz *Ann. Phys., Lpz.* **2** 55
[19] Wylie J M and Sipe J E 1984 Quantum electrodynamics near an interface *Phys. Rev.* A **30** 1185
[20] Ford G W and Weber W H 1984 Electromagnetic interactions of molecules with metal surfaces *Phys. Rep.* **113** 195
[21] Azoulay J, Débarre A, Richard A and Tchénio P 2000 Quenching and enhancement of single-molecule

fluorescence under metallic and dielectric tips *Europhys. Lett.* **51** 374
[22] Ayars E J, Hallen H D and Jahncke C L 2000 Electric field gradient effects in raman spectroscopy *Phys. Rev. Lett.* **85** 4180
[23] Feibelman P J 1975 Microscopic calculation of electromagnetic fields in refraction at a jellium–vacuum interface *Phys. Rev.* B **12** 1319
[24] Larkin I A, Stockman M I, Achermann M and Klimov V I 2004 Dipolar emitters at nanoscale proximity of metals surfaces: giant enhancement of relaxation in microscopic theory *Phys. Rev.* B **69** 121403(R)
[25] Castanié E, Boffety M and Carminati R 2009 Non-local interactions in single-molecule fluorescence close to metal surfaces, in preparation
[26] Sipe J E 1987 New Green-function formalism for surface optics *J. Opt. Soc. Am.* B **4** 481
[27] Purcell E M and Pennypacker C R 1973 Scattering and absorption of light by non-spherical dielectric grains *Astrophys. J.* **186** 705
[28] Tsang L, Kong J A, Ding K-H and Ao C O 2001 *Scattering of Electromagnetics Waves: Numerical Simulations* (New York: Wiley)
[29] Paulus M and Martin O J F 2001 Light propagation and scattering in stratified media: a Green's tensor approach *J. Opt. Soc. Am.* A **18** 854
[30] Palik E W 1985 *Handbook of Optical Constants of Solids* (San Diego, CA: Academic)
[31] Carminati R, Nieto-Vesperinas M and Greffet J-J 1998 Reciprocity of evanescent electromagnetic waves *J. Opt. Soc. Am.* A **15** 706